ELSEVIER

Physica A 301 (2001) 375–396

PHYSICA A

www.elsevier.com/locate/physa

Multifractal random walk in copepod behavior

François G. Schmitt[a,*], Laurent Seuront[b]

[a] *Department of Fluid Mechanics, Vrije Universiteit Brussel, Pleinlaan 2, B-1050 Brussels, Belgium*
[b] *Ecosystem Complexity Research Group, Station Marine de Wimereux, CNRS UPRESA 8013 ELICO, Université des Sciences et Technologies de Lille, 28 avenue Foch, BP 80, F-62930 Wimereux, France*

Received 20 August 2001

Abstract

A 3D copepod trajectory is recorded in the laboratory, using two digital cameras. The copepod undergoes a very structured type of trajectory, with successive moves displaying intermittent amplitudes. We perform a statistical analysis of this 3D trajectory using statistical tools developed in the field of turbulence and anomalous diffusion. We show that the walk belongs to "multifractal random walks", characterized by a nonlinear moment scaling function for the distance versus time. To our knowledge, this is the first experimental study of multifractal anomalous diffusion in natural sciences. We then propose a new type of stochastic process reproducing these multifractal scaling properties. This can be directly used for stochastic numerical simulations, and is thus of important potential applications in the field of animal movement study, and more generally of anomalous diffusion studies.

PACS: 87.10.+e; 92.20.Rb; 47.53.+n; 05.40.+j

Keywords: Animal behavior; Plankton; Anomalous diffusion; Multifractals; Random walks; Stochastic processes

1. Introduction

For most animals, movement behavior determines how individuals encounter features of their environments that vary in time and in space. Space–time variability in such ecological phenomena as foraging behavior, mating probabilities, population distribution, metapopulation dynamics, predator–prey or parasitoid–host interactions, or community composition may therefore be mechanistically determined by how individual movement behavior is influenced by space–time heterogeneity in environmental features [1–3].

* Corresponding author. Tel.: +32-2-6292334; fax: +32-2-6292880.
E-mail address: francois@stro.vub.ac.be (F.G. Schmitt).

0378-4371/01/$ - see front matter
PII: S0378-4371(01)00429-0

For zooplankton, competition, predation and aggregation occur across distances of centimeters to meters. However, the consequences of these interactions influence processes such as climate and fisheries productivity up to the global scale [4–6]. In this context, and considering the extremely intertwined properties of swimming and feeding processes in copepods ecology [7], testing mechanistic hypotheses that relate individual movements to higher level ecological phenomena requires that individual swimming pathways be precisely characterized, both qualitatively and quantitatively.

In the following, we first propose a state of the art in animal behavior studies, in both terrestrial and aquatic studies (Section 2). We present our choice of copepod species and experimental procedure in Section 3. Section 4 presents our statistical analysis of copepod swimming behavior. We experimentally show for the very first time that copepod display a multifractal random walk, whose statistics are characterized by a nonlinear scaling exponent for the statistical moments of the increment of position. We also show that successive displacements display long-range power-law correlations, invalidating the usual uncorrelated random walk hypothesis. In Section 5 we discuss the consequences of our findings and propose a new scaling stochastic process that reproduces the nonlinear scaling moment function for the displacements. In Section 6 we give some final comments and directions of future developments.

2. Some previous animal behavior studies

2.1. Characterizing movement pathways

Movement pathways have been characterized by a variety of measures, including path length (the total distance traveled or gross displacement), move length (the distance traveled between consecutive points in time), move duration (time interval between consecutive spatial points), speed (move length divided by move duration), turning angle (the difference in direction between two successive moves), turning rate (turning angle divided by move duration), net displacement (the linear distance between starting and ending point), often used as a metric when making comparisons with diffusion or correlated random walk models [8,9], Net to Gross Displacement Ratio (NGDR) [10] and fractal dimension [11,12]. These different metrics have been widely applied in both terrestrial and aquatic ecology. In Sections 2.2 and 2.3, we briefly exemplify the main ecological conclusions drawn from behavioral studies in both terrestrial and aquatic ecology.

2.2. Movement pathways in terrestrial ecology

Characterizing the movement of organisms has a long lasting history [1], and a profusion of applications are found in entomological studies [2]. More specifically, Brownian and fractional Brownian motion models [12] have been proposed to mimic insect motions in a variety of environments. Dicke and Burrough [13] used fractal

analysis to examine spider mite movements in the presence and absence of a dispersing pheromone. Following a different approach, Wiens and Milne [14] examined beetle movements in natural fractal landscapes. They found that observed beetle movements deviated from the modeled (fractional Brownian) ones. A follow-up study [9] found that beetle movements reflect a combination of ordinary (random) and anomalous diffusions. The latter may simply reflect intrinsic departures from randomness, or result from barrier avoidance and utilization of corridors in natural landscapes. Johnson et al. [15] discuss the interaction between animal movement characteristics and the patch-boundary features in a 'microlandscape'. They argue that such interactions have important spatial consequences on gene flow, population dynamics and other ecological processes in the community [16]. In a comparison of path tortuosity in three species or grasshopper, With [17] found that the path fractal dimension of the largest species was smaller than those of the two smaller ones. She suggested that this reflects the fact that smaller species interact with the habitat at a finer scale of resolution than do larger species. A subsequent study [18] showed differences in the ways that gomphocerine grasshopper nymphs and adults interacted with the microlandscape.

Following the development of observational methods such as radio-telemetry [19], similar studies have been conducted to characterize the search paths of small [19–22] and large [23–25] mammals. These behavioral studies then provided salient information to identify specific food search-strategies from local to global scales. For instance, finch flocks tend to move forward rather than turn to the side, and almost never turned backward [20], red foxes move during the night and remain relatively stationary during the day [19] and wolf females movement paths show significant changes throughout the year, depending on the state of their life cycle (normal, breeding and wandering) [23]. Similar studies are also essential to discriminate between (i) acquired behavior, perceptible from the spatial memory of vervet monkeys who appear to behave as though they can "look ahead" at least three steps and thus might use a permutational heuristic to solve spatial foraging problems [21], and (ii) inborn behavior related to straighter movements of caribou during their annual migrations [25].

2.3. *Movement pathways in aquatic ecology*

Despite a fast growing number of studies, analyses of movement behavior of organisms are less common in aquatic than in terrestrial organisms, primarily because of the difficulty in obtaining accurate records of the displacement of swimming organisms, which unlike terrestrial organisms, take place through a volume and therefore require systems capable of recording three-dimensional (3D) data. Taking advantages of the recent improvements of radio-telemetry technology, approaches devoted to study the behavior of large animals, such as sharks [26,27], tuna [28], sea turtles [29], seals [30] or marine birds [31–33], showed an important development in the last 10 years. It is now feasible to obtain records down to several hundreds of meters, over wide geographic areas and for several months.

On the other hand, behavioral studies of smaller animals such as tiny fishes, crabs and plankton organisms required the use of sophisticated in situ [34,35] and laboratory [36] video system. Examples are obtained from the wide spectrum of swimming behaviors related to the species [37], the age [38–41], the prey density [42–44], the presence of a predator or a conspecific [41,45,46], the sex of individuals [39,47,48], the information imparted into the surrounding water by a swimming animal [49,50], including both chemical [51,52] and hydromechanical [47,53–56] stimuli. In particular, as widely demonstrated for terrestrial organisms, zooplankton organisms are now recognized to present behavioral adaptation to resource patchiness: they increase [39] or decrease [42,43,57] their swimming speed with increasing phytoplankton densities, i.e., a species-specific adaptation to increase the encounter rate with their preys, and increase the tortuosity of their swimming paths in food patches [57–60].

However, one needs to note here that the development of such video recording apparatus is a nontrivial problem, especially in plankton ecology, and has resulted in many investigations of zooplankton behavior recording only two-dimensional (2D) swimming pathways. Moreover, even using video systems capable of recording 3D data, there are still problems of scale resulting from the small size of planktonic organisms. Gathering 3D coordinates for zooplankton involves a trade-off between resolution and extent, typically presenting researchers with two alternatives in the collection of data: (i) high spatial resolution, but for short duration, or (ii) longer time series, but at low spatial resolution. To our knowledge, only two studies have permitted the collection of 3D swimming data at both high spatial resolution and for long periods [38,43]. We then present in the following an alternative, original and simple procedure to acquire reliable 3D data of the swimming behavior of zooplankton organisms.

3. Recording 3D behavior of swimming organisms

3.1. Living material collection and acclimation

The copepods are the largest and most diversified group of crustaceans, and are the most numerous metazoans (i.e., all multicelled organisms) in the aquatic communities. At present, they include over 14,000 species, 2300 genera and 210 families, a surely underestimated number. Their habitat ranges from fresh water to hyper-saline conditions, from subterranean caves to water collected in bromeliad leaves or leaf litter on the ground, from streams, rivers and lakes to the sediment layer in the open ocean, from the highest mountains to the deepest ocean trenches and from the cold polar ice–water interface to the hot active hydrothermal vents. Copepods may be free-living, symbiotic, or internal or external parasites on almost every phylum of animals in water. The usual length of adults is 1–2 mm, but adults of some species may be as short as 0.2 mm and others may be as long as 10 mm. They are considered the most plentiful multicultural group on the earth, outnumbering even the insects, which include more species, but fewer individuals. Particularly, the copepods are the dominant forms of the

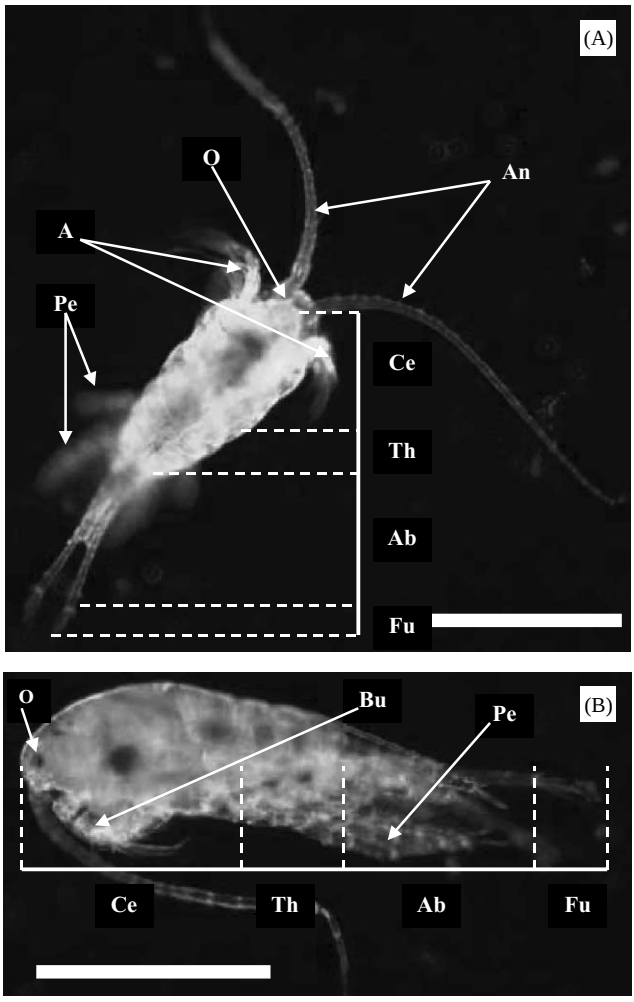

Fig. 1. Dorsal (A) and side (B) view of the copepod *Temora longicornis*. Antennules (An) and antennae (A) hold chemo- and mechano-receptors used to scan the surrounding environment. The cephalothorax (Ce) holds a rudimentary eye, the ocellus, and the mouth appendages (Bu) (mandibles, maxillules and maxillae) responsible for the capture and handling process of food particles. The thorax holds biramous swimming legs, the peraeopod (Pe). The abdomen (Ab) and the furca (Fu) do not hold any appendages, while the former holds the genital apparatus. The scale bars represent 0.5 mm.

marine plankton, that constitute the secondary producers in the marine environments and then a fundamental step in the oceanic food chain, linking microscopic algal cells to juvenile fishes and whales. Copepods also have the potential to act as control mechanisms for malaria by consuming mosquito larvae, and contrarily are intermediate hosts of many human and animal parasites.

In this preliminary study, we focused on the calanoid copepod *Temora longicornis* (Fig. 1), a very abundant species in worldwide coastal waters, which is also of great

ecological significance in many areas. For instance, it represents 35–70% of the total copepod population in the southern Bight of the North Sea [61], and in Long Island Sound, USA, *T. longicornis* has been shown to be able to remove up to 49% of the daily primary production [62]. Feeding and swimming being two intertwined processes in copepods ecology, the precise characterization of the swimming behavior represents a salient issue in marine ecology.

Individuals of the copepod *T. longicornis* were collected with a WP2 net (200 mesh size) in the offshore waters of the Eastern English Channel. Specimens were diluted in buckets and transported to the laboratory. The acclimation of copepods consisted of being held in 20 l beakers filled with 0.45 μm filtered seawater to which was added a suspension of the diatom (a phytoplankton algae) *Skeletonema costatum* to a final concentration of 10^8 cells l^{-1}. Prior to the filming experiment, adult females were sorted by pipette, acclimated for 24 h at 18°C and fed on a mixture of the green algae *Nannochloropsis occulata* (3 μm) and the flagellate *Oxyrrhis marina* (13 μm). The larger heterotrophic flagellate *O. marina* was present as an additional food source. In this preliminary experiment, an adult female (1.1 mm) was sorted by pipette and left in the experimental filming setup to acclimatize for about 15 min prior to filming. A realistic concentration of the mixture of *N. occulata* and *O. marina* was tested: *N. occulata* and *O. marina* at 10^8 and 10^6 cells l^{-1}, respectively.

3.2. Experimental design

The experimental setup (Fig. 2) was designed to track the 3D displacement of a copepod in a cubic glass container (inner side 15 cm, effective volume 3.375 l). Illumination came from two lamps (diffuse cold light 75 W) located above and below the container to ensure homogeneity of the light source and thus to avoid phototropism. Reflections were minimized as much as possible and two lateral sides of the container were covered with black dull plastic film to increase the contrast between the copepod and the container background.

The 3D trajectory of the copepod was recorded using two orthogonally focused and synchronized CCD cameras (HITACHI KP M1; 875×560 pixels; focal distance 17 : 53 mm), facing the two observations frames of the experimental container. The cameras deliver black and white frames at a rate of 12.5 frames per second, and rulers provide the relation between pixels and millimeters. An encoder RGB-PAL [Enc110 (For-A)] codes PAL-type red and green frames from the two instantaneous synchronized monochrome images. Each orthogonal view then gets an identity and may be added to another at the same time t to form one single color PAL-frame. In particular, this frame's superposition reduces hardware cost and gives a perfect synchronization. The color images were digitized (720×576 pixels), compressed and stored in real time using a special acquisition card and an appropriate software (PVR-Digital Processing Systems) on a PC.

Finally, the three components of the copepod trajectory were extracted using frame analysis. A pre-recorded background was removed from each frame, leading to a

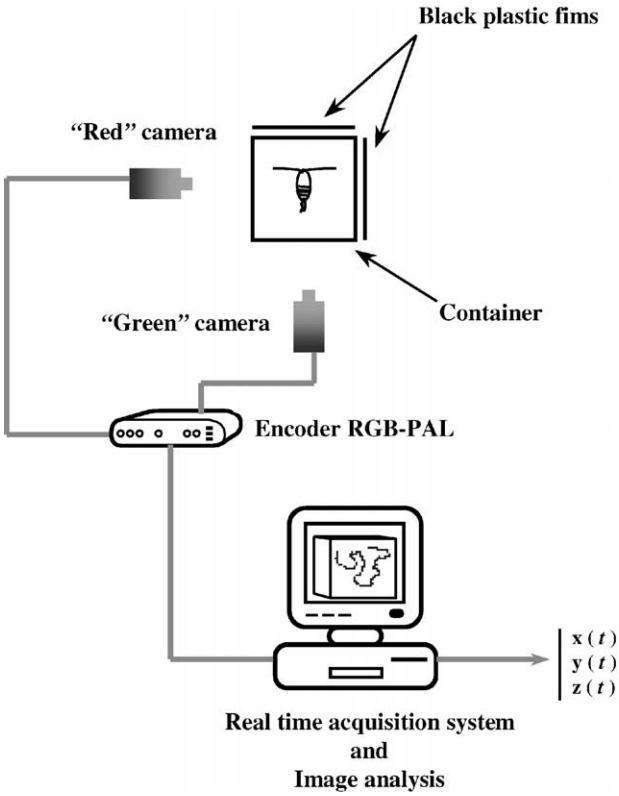

Fig. 2. Schematic representation of the data acquisition system. The copepod is kept in a cubic glass container, and its swimming pathway is recorded using two synchronized and orthogonally focused cameras. After encoding of the two instantaneous synchronized images, the three components of the copepod trajectory were extracted using frame analysis.

decomposition of the initial colored frames into gray-level frames giving two binary frames by thresholding. After a morphological opening to filter parasitic points, each binary frame is labeled to get the coordinates (in the image system) and the objects numbered on it. This frame processing was carried out on the acquisition PC (Pentium Pro 200 MHz) at a rate of 1.5 s per frame. An identification software subsequently eliminates spurious objects (i.e., ludicrous discontinuities in the trajectory). Another software takes into account spatial parallax and diffraction phenomena and gives the three coordinates of the copepod as a function of time in the container coordinates system. While the frame-disk is able to store about 40 min of a series at 12.5 images per second, we only recorded the swimming behavior of the *T. longicornis* individual for 7 min, after which the 3D trajectory was reviewed and valid segments were identified for analysis. Valid segments consisted of pathways in which the animals were swimming freely, at least two body lengths away from any of the chamber's walls or the surface. In a further analysis, we use the longer (i.e., 2 min 42 s) valid segment available from our lab experiment.

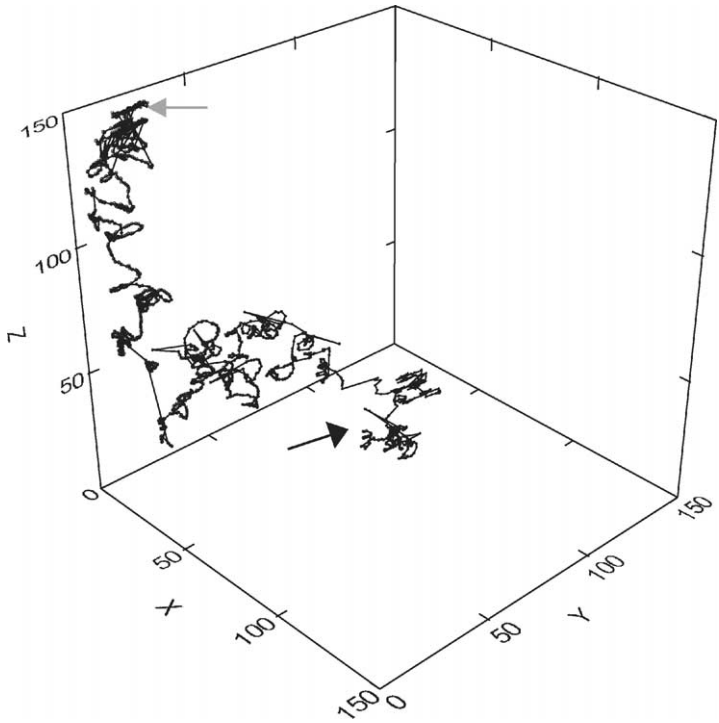

Fig. 3. Three-dimensional swimming pathway of the copepod *Temora longicornis*. *T. longicornis* moved actively in a highly variable and irregular pathway, showing an alternation between periods of relative straight swimming and periods of erratic motions including strong jumps in all three dimensions. The black and gray arrows indicate the beginning and the end of the swimming path, respectively.

3.3. Behavioral observations

The 3D record of the swimming behavior of *T. longicornis* is shown in Fig. 3. *T. longicornis* moved actively in a highly variable and irregular pathway, showing an alternation between periods of relative straight swimming and periods of erratic motions including strong jumps in all three dimensions, ensuring the 3D nature of the recorded pathway. Both the qualitative and quantitative nature of these fluctuations will be investigated in Section 4 using an original statistical procedure.

4. Statistical analysis of the copepod displacements

Strictly speaking, planktonic organisms are passively advected by the surrounding water masses, or present swimming abilities that are negligible when compared to the amplitude of turbulent motions. In practice, copepod displacements result of their own movements, that must be added to the advective motions generated by oceanic

turbulence. Here, we specifically study copepod movements without turbulence, in order to be able to directly characterize its specific movement ability and to establish a biological reference framework, before considering more complex situations where the physical effects of turbulence affect biological properties. As we shall see, contrary to what could be believed, not only copepods are able to swim very fast relative to their size and to the turbulence levels they experience in the field, but they also produce a very structured type of movement.

After comparing copepod swimming velocity and turbulent characteristic velocity, we analyze here the statistics of copepod displacements using an original approach derived from the field of anomalous diffusion. We first characterize the multifractal properties of 3D copepod displacements, then consider their 2D projections. We further analyze the statistics of successive displacements: their amplitudes and angles.

4.1. Copepod swimming speed and turbulence

We present here a brief comparison between the swimming ability of the copepod *T. longicornis* and the turbulent velocity relevant at their characteristic scale. The root-mean-square turbulent velocity w (referred to as rms turbulent velocity hereafter) at a scale d writes $w = C\varepsilon^{1/3}d^{1/3}$, where C is a constant and ε ($m^2\ s^{-3}$) is the small-scale turbulent dissipation rate belonging to the inertial subrange. At the scale of a plankton organism l (m), the most relevant turbulent velocity can then be expressed as [63]

$$w = 1.37\varepsilon^{1/3}l^{1/3}\,. \tag{1}$$

Here, considering the characteristic scale $l = 1.1$ mm (i.e., the body length of the copepod), we estimate the rms turbulent velocity w for different values of the dissipation rate ε ranging between 10^{-10} and $10^{-4}\ m^2\ s^{-3}$. Values bounded between 10^{-10} and $10^{-6}\ m^2\ s^{-3}$, 10^{-7} and $10^{-6}\ m^2\ s^{-3}$ and 10^{-6} and $10^{-4}\ m^2\ s^{-3}$ are characteristic of the open ocean, the continental shelf and highly dissipative coastal waters, respectively. It can be seen from Fig. 4 that the observed swimming velocity v of *T. longicornis*, i.e., $v = 1.3\ mm\ s^{-1}$, is larger than the rms turbulent velocity observed in most marine environments. Indeed, the rms velocity overcomes the swimming velocity of the copepod *T. longicornis* only for very high values of the dissipation rates ε ($\varepsilon \geqslant 10^{-5}\ m^2\ s^{-3}$) characterizing extremely turbulent environments such as breaking waves or narrow tidal channels. However, the maximum swimming velocity, i.e., $v = 29.0\ mm\ s^{-1}$, is significantly higher (an order of magnitude) than the rms turbulent velocity observed in the highest turbulent marine areas. These very simple arguments then demonstrate that the concept of "plankton" is all relative and should be used very carefully even when applied to swimming animals as tiny as copepods.

4.2. Multifractal study of copepod displacements

We note here $\mathbf{X}(t)$ the 3D position of the copepod at time t. We consider the norm of its displacements $\Delta\mathbf{X}_\tau = \mathbf{X}(t+\tau) - \mathbf{X}(t)$: by hypothesis, the moments of order

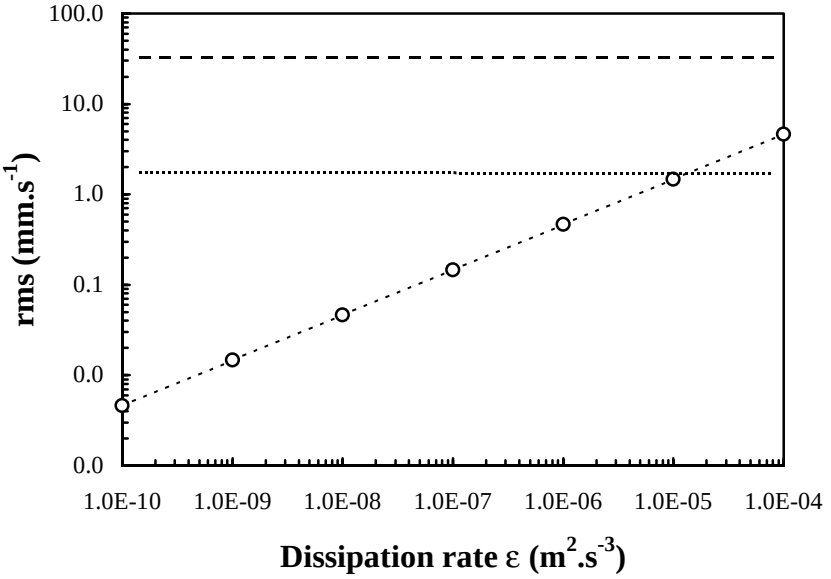

Fig. 4. Log–log plots of the root-mean-square turbulent velocity w (mm s^{-1}) estimated at the copepod characteristic scale (1.1 mm) as a function of the dissipation rate of turbulent kinetic energy ε (m^2 s^{-3}). The dotted and dashed lines correspond to the mean and maximum swimming speed of the copepod *Temora longicornis*, $v = 1.3$ mm s^{-1} and $v = 29.0$ mm s^{-1}, respectively, as observed in our lab experiment.

$q > 0$ of the displacements depend only on the time increment τ. In case of scaling, we introduce the moment function exponent $\zeta(q)$ defined as [64–73]

$$\langle \|\Delta \mathbf{X}_\tau\|^q \rangle \approx \tau^{\zeta(q)} . \tag{2}$$

This exponent function is very useful to characterize the statistics of the random walk. For the Brownian motion, it is well-known that $\zeta(q) = q/2$. Classically, only the moment of order 2 is estimated, and whenever $\zeta(2) = 1$, the process corresponds to a normal diffusion, whereas the rich field of anomalous diffusion corresponds to dispersive processes with $\zeta(2) \neq 1$ (see reviews on anomalous diffusion in Refs. [74,75]). The idea behind this characterization using only one moment was to assume implicitly that if $\zeta(2) = 1$, one has for all q's $\zeta(q) = q/2$, then the process has the same diffusive properties as Brownian motion. Of course, this is not necessarily the case, and one can have $\zeta(2) = 1$ (so that the diffusion is apparently normal, see an example in Ref. [76]), whereas for other moments $\zeta(q) \neq q/2$. It is thus better to characterize the process with the whole function $\zeta(q)$ instead of a single exponent, as done in Refs. [64–73]. In this framework, it would be more coherent to denote "anomalous diffusion" as a diffusion with a function $\zeta(q) \neq q/2$.

When the function $\zeta(q)$ is nonlinear, we refer the resulting diffusion as being "multifractal", by analogy with multifractal characterization of correlations and intermittency in turbulence (see Refs. [77,78] for recent reviews). The terms "multifractal random walk" were already proposed in Ref. [73]. Before this, a diffusion characterized by a

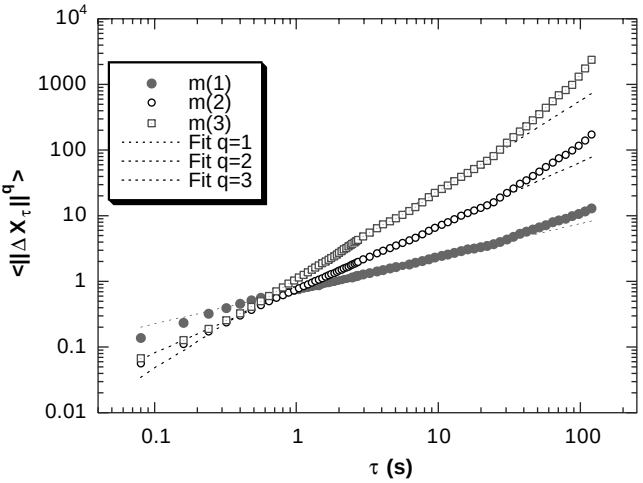

Fig. 5. The moments $\langle \|\Delta \mathbf{X}_\tau\|^q \rangle$ vs. τ for $q = 1, 2, 3$. A very agreeable scaling behavior is visible on 2 decades, for temporal increments between 0.3 and 30 s.

nonlinear $\zeta(q)$ function has received different names: generalized diffusion [64], multi-diffusion [66], multifractional kinetics [67,68], or strong diffusion [69–72].

We first analyzed the 3D trajectory of the copepod movements shown in Fig. 3. The scaling of several moments is shown in Fig. 5. It can be seen that the scaling is very good for a range of scales of 2 decades, for times between 0.3 and 30 s, corresponding to distances between 0.4 and 4 cm (the distance varies with the square-root of time, so that a time ratio of 100 corresponds to a distance ratio of 10). For smaller distances, the departure from scaling could be due to the reaction time of the copepod. In order to precisely detect a departure from normal diffusion, this scaling behavior is displayed in Fig. 6 with a compensation by the normal diffusion scaling exponent: this shows the anomalous diffusion obtained for the range of scales presented above. It can be seen that $\zeta(2)$ is slightly smaller than 1, with a very small correction; the correction is larger for $q > 3$. In the following, scaling exponents are estimated as a least-squares power-law slope. Fig. 7 shows the resulting $\zeta(q)$ function, which is clearly nonlinear. The straight line of equation $q/2$ is shown for comparison. For moments larger than 2, the departure from this straight line is very clear. The function obtained is nonlinear and convex, as opposed to the numerical studies presented in Refs. [69–71], where the same function is bilinear and concave. This characterizes different types of anomalous diffusion.

We also compare the functions obtained in three dimensions with the scaling exponents estimated from 2D projections in the xy, xz and yz planes. This can be useful for comparison with other data bases where only two coordinates are recorded. For example, a numerical study in two dimensions has been performed in Ref. [76], where the copepod was assumed to diffuse in a multifractal phytoplankton field. Fig. 8 shows that the $\zeta(q)$ functions estimated from 2D data have the same shape as the original 3D

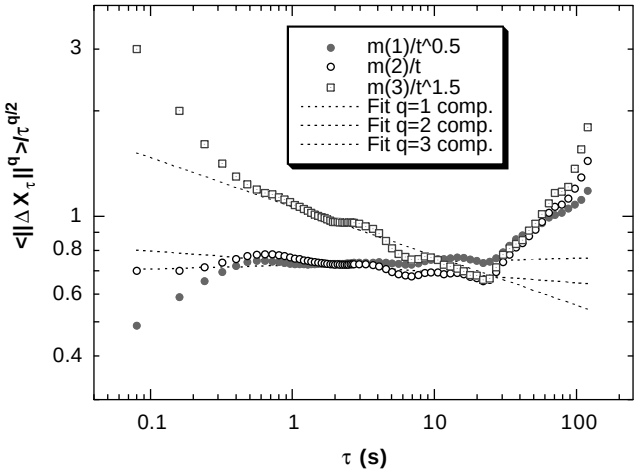

Fig. 6. The compensated moments $\langle \|\Delta \mathbf{X}_\tau\|^q \rangle / \tau^{q/2}$ vs. τ for $q = 1,\ 2,\ 3$. A scaling of the residual indicates anomalous scaling diffusion, which is confirmed by the visible trends for the same temporal increments as Fig. 4.

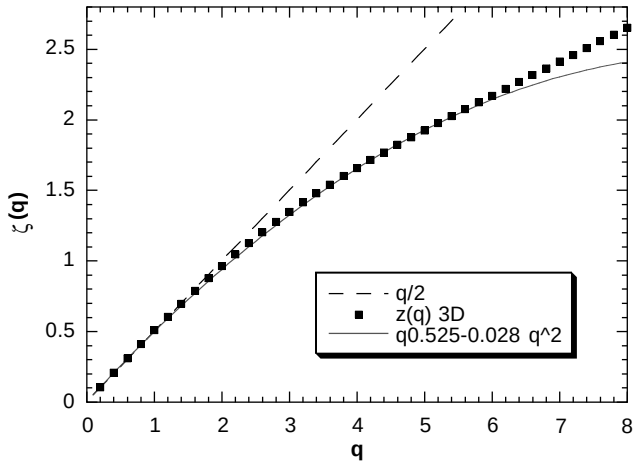

Fig. 7. The function $\zeta(q)$ experimentally determined from the data (dark squares), compared to a fit corresponding to normal diffusion ($q/2$, dotted line) and a nonlinear multifractal fit (continuous line).

one, with some statistical variations which are expected to be due to the finite size of the data base.

4.3. *Analysis of successive displacements*: *amplitudes and angles*

Here, we perform some complementary analysis, helping to provide some general understanding of the structure of the copepod random walk. We consider the "moves" as the difference in position of the copepod for time increments of 0.08 s (the resolution

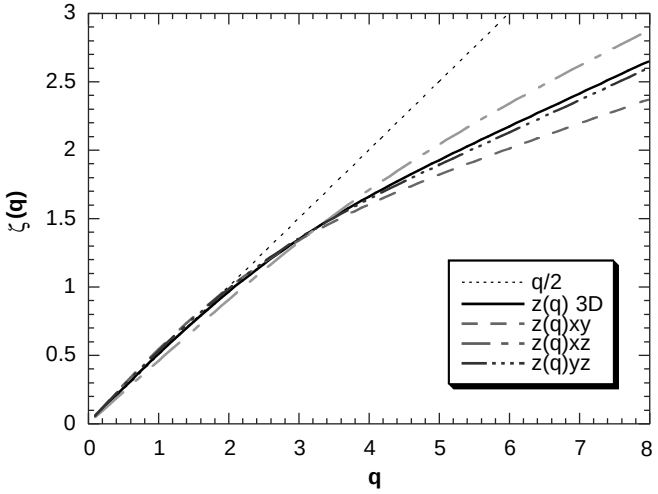

Fig. 8. The function $\zeta(q)$ experimentally determined from 3D data, compared to the functions estimated from 2D projections in the xy, xz and yz planes, respectively.

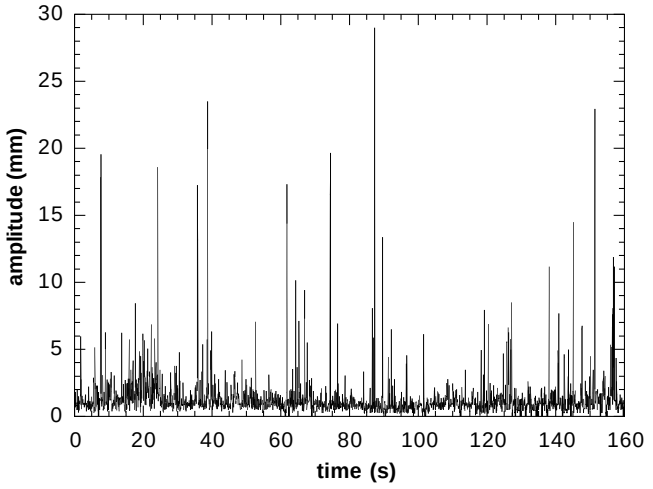

Fig. 9. The series of amplitudes of successive moves showing an intermittent structure.

time step). We consider the structure of these elementary moves: the correlation of their amplitude and the angle between successive moves.

We display the successive move amplitudes in Fig. 9. It can be seen that the moves are very intermittently distributed, with some large ones separated by very small ones. This time series has a specific structure, recalling the fields resulting from direct multiplicative cascades (see Ref. [77]). Its correlation function, represented in Fig. 10, shows a long-range power-law correlation. This behavior is in agreement with the

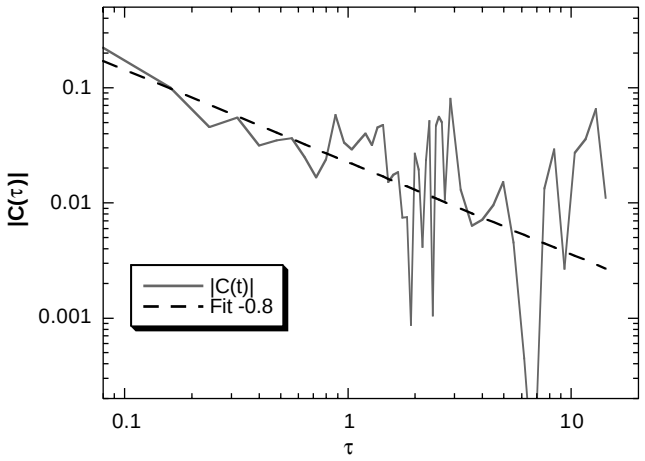

Fig. 10. Autocorrelation function of the series of successive moves confirming the long-range correlations of the displacements.

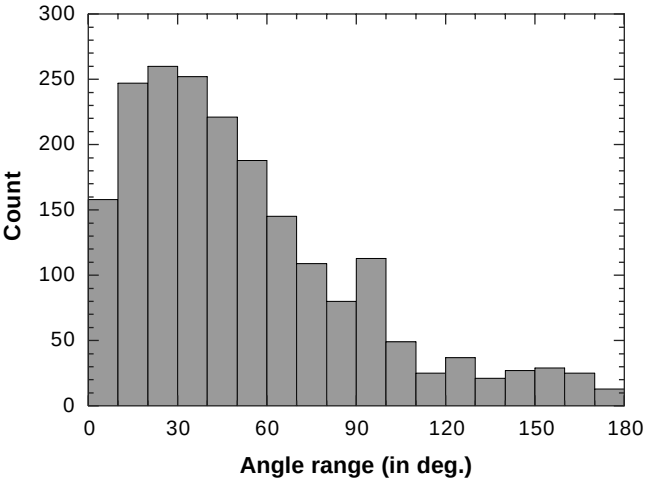

Fig. 11. Histogram of the angle between successive displacements. The copepod sometimes moves backward. There is a local maximum at a nonzero angle of about 20°.

nonlinearity of the $\zeta(q)$ function. We also considered the angle between successive moves. No correlation could be detected between the angle and the amplitude of moves. The angles themselves are not equally probable: Fig. 11 shows their histogram, indicating as expected, that angles $> 90^{\circ}$ are less probable: the copepod moves more likely forward than backward. Nevertheless, it moves sometimes backward, and the histogram shows that a local maximum is obtained for angles of about 20°: the copepod moves more likely ahead with a small deviation in angle. These are interesting

characterizations that could be taken into account when simulating copepod behavior in e.g. multiagent type of simulations [79].

5. Discussion and proposal of a new scaling stochastic process

We have obtained the above experimental evidence of anomalous diffusion for 3D data, with multifractal statistics. For theoretical as well as numerical developments of these results, the question then arises as to how to formalize or simulate stochastic processes possessing such multifractal random walk properties. We discuss here briefly this question. We first provide a general framework possessing the required multiscaling statistics, then we discuss possible stochastic kernels available. We also discuss other published results in the same direction.

5.1. Stochastic processes for multifractal random walks

Let us consider first the 1D case. Possible 3D generalizations will be discussed elsewhere. Let us consider a stochastic kernel $f(t,s)$ possessing the following properties:

$$f(at,as) \stackrel{\mathrm{d}}{=} g(a) f(t,s), \quad a>0\,, \tag{3}$$

where '$\stackrel{\mathrm{d}}{=}$' means equality in distribution, and $g(t)$ is a nonstationary random process characterized by its moments $q>0$:

$$\langle |g(t)|^q \rangle = t^{-\psi(q)}, \quad t>0\,, \tag{4}$$

where $-\psi(q)\ln t$ is its second Laplace characteristic function, that is assumed to converge (at least for some moments $q>0$). We consider here (3) and (4) as granted, and discuss how to build such process in Section 5.2.

We then define the random walk as follows:

$$X(t)-X(0) = \int_0^t f(t,s)\,\mathrm{d}B(s)\,, \tag{5}$$

where $B(t)$ is a Brownian motion. When $f=1$ (nonrandom), this recovers the classical random walk for $X(t)$. In the general case, this walk possesses the following scaling:

$$\begin{aligned} X(at)-X(0) &= \int_0^{at} f(at,s)\,\mathrm{d}B(s)\,, \\ &= \int_0^t f(at,as')\,\mathrm{d}B(as'), \quad (s'=s/a) \\ &\stackrel{\mathrm{d}}{=} \int_0^t g(a) f(t,s') a^{1/2}\,\mathrm{d}B(s')\,, \\ &\stackrel{\mathrm{d}}{=} g(a) a^{1/2}(X(t)-X(0))\,. \end{aligned} \tag{6}$$

When taking $t=1$ fixed and a as variable, and taking the moments of order $q>0$ of each side, one obtains

$$\langle |\Delta X(a)|^q \rangle = C_q a^{q/2} \langle |g(a)|^q \rangle \approx a^{\zeta(q)}\,, \tag{7}$$

where C_q is a constant and

$$\zeta(q) = \frac{q}{2} - \Psi(q) . \tag{8}$$

We then discuss how to obtain conditions (3) and (4) with a nonlinear function $\Psi(q)$.

5.2. Scaling stochastic kernels

Let us consider $x(t)$ a process with stationary independent increments such as $x(0) = 0$. Then for $\tau > 0$ it is well-known that $y_\tau(t) = x(t+\tau) - x(t)$ is an infinitely divisible stochastic process (see, e.g. Ref. [80]). Introducing—when defined—the second Laplace characteristic function

$$\Psi_{y_\tau}(q) = -\log\langle e^{q y_\tau(t)}\rangle \tag{9}$$

one has

$$\Psi_{y_\tau}(q) = \tau \Psi_{y_1}(q) . \tag{10}$$

This may be rewritten as

$$\langle e^{qx(t)}\rangle = e^{-t\psi(q)} , \tag{11}$$

where $\Psi(q) = \Psi_{y_1}(q)$. Let us introduce $g(t) = e^{x(\log t)}$. The moments of this process thus satisfy

$$\langle g(t)^q\rangle = \langle e^{qx(\log t)}\rangle = t^{-\psi(q)} , \tag{12}$$

so that one has for $a > 0$,

$$g(at) \stackrel{d}{=} g(a)g(t) . \tag{13}$$

Now, taking $f(t,s) = g(|t-s|)$ for $t \neq s$, one obtains a stochastic kernel $f(t,s)$ satisfying relations (3) and (4), where $\Psi(q)$, as the second Laplace characteristic function of an infinitely divisible random variable, is a nonlinear and convex function.

This shows that any infinitely divisible probability distribution can be used as a basis of the stochastic kernel $f(t,s)$ used to introduce a multifractal random walk. Let us mention among possible kernels the Poisson process, or the Levy stable family, among which the Gaussian process is present. In the latter case, one has $\Psi(q) = Cq^2$, so that a possible form of $\zeta(q)$ would be

$$\zeta(q) = \frac{q}{2} - Cq^2 . \tag{14}$$

In Fig. 7, a fit of the experimental curve of the form $\zeta(q) = Aq - Cq^2$ was performed, with $A = 0.525$ and $C = 0.028$, shown for illustration. This provides a very good fit until a moment of order 6, which is already high for such a small data set. This is shown only for illustration purpose: it could well be that the multifractal diffusion is driven by another type of stochastic kernel (such as log-stable): there are too few data available to investigate this point here.

5.3. Comparison with other proposals

There have been several interesting proposals in the literature to simulate multifractal fields having the same scaling properties as turbulent velocity: Juneja et al. [81] have proposed a discrete (in scale) decomposition, and Biferale et al. [82] a discrete (in scale) but causal process, that could be adapted to simulate a discrete multifractal random walk. These models possess discrete dilatation invariance, while Bacry et al. [73] have introduced a multifractal random walk model possessing continuous dilatation invariance properties. Nevertheless, they could only propose explicitly a discrete version of this model: they showed that the model is not ill-defined in the continuous limit, but could not provide the corresponding stochastic process. Furthermore, their approach corresponds only to the Gaussian case, while our proposal is more general, since it involves the whole infinitely divisible family. Apart from these differences, the approach in Ref. [73] seems to be in the same direction as our proposal: a Gaussian stochastic integral with an independent stochastic kernel.

Our multifractal random walk model was presented here as an illustration of a process able to reproduce the main statistical properties shown by the data; a more detailed study of its properties will be discussed elsewhere.

6. Concluding remarks

Let us summarize here the main results of this paper, and briefly discuss their potential implications. We have presented a 3D data base of a copepod random walk in a nonturbulent environment, and shown its multifractal characteristics. The present data base concerned only one realization, with 2 min and 42 s of data recorded at 12 Hz. In particular, the results presented here have several potential implications on our understanding of zooplankton behavior and trophodynamics. For instance, is the observed behavior an inborn property, or is a specific response induced by the environment?

In this way, one needs to note that the behavior observed here could be related to the heterogeneous nature of phytoplankton distribution in the experimental container. After being introduced in the cubic container, phytoplankton cells have been stirred by turbulent mixing. This turbulent mixing may well have produced a multifractal distribution of phytoplankton (see e.g. Ref. [83] for a multifractal study of the heterogeneous distribution of phytoplankton in the ocean). The container was then maintained at rest for 15 min before the introduction of the copepod, so that the heterogeneous distribution is homogenized by molecular diffusion. A characteristic time scale of 15 min corresponds to scales homogenized by molecular diffusion up to 3 cm, which is similar to the largest scale of our anomalous scaling range. The observed multifractal random walk then occurred over a range of scales where phytoplankton distribution is thought to be homogenized, and could not be related to a heterogeneous distribution of phytoplankton cells. This result rather suggests an inborn than an induced behavior.

On the other hand, the potential identification of different modes in the swimming behavior of *T. longicornis* (cf. Fig. 8) in the vertical and the horizontal dimensions may reflect (i) the effect of gravity which affects most copepod species and *T. longicornis* in particular [36], and/or (ii) an adaptive reminiscence of diel vertical migration as a predator avoidance strategy [84], and/or (iii) a feeding switch between two different kinds of food sources as the nonmotile alga *N. occulata* and the motile flagellate *O. marina* used in the present study. Differential swimming behaviors in the horizontal and the vertical planes may also be suggested as a potential basis to investigate the predation risk associated with the differential swimming behavior related to mating, feeding or predator avoidance strategies.

Whatever that may be, the full understanding of the very structured nature of the copepod's movements needs further experimental work. In particular, a comparison of the behavior of different species of copepods will be done in the framework introduced here, as well as a study of the influence of the feeding conditions (i.e., quality and quantity of food) on the statistics of the walk. Moreover, let us note that a multifractal characterization of copepod spatial distribution has already been demonstrated in another context in turbulent oceanic conditions [85,86]. Further studies could then, in particular, be able to relate the statistics of copepod diffusion in real conditions with those of the spatial density of copepods (i.e., to relate Lagrangian diffusion with the resulting spatial statistics) as previously suggested in terrestrial ecology [8].

These results were, to our knowledge, the first experimental evidence of multifractal anomalous diffusion in natural sciences (finance excluded): all the previous studies on this topic seem to be either theoretical or numerical simulations of different deterministic or stochastic diffusion models.

These results characterize copepod diffusion in the absence of turbulence. It provides preliminary information that can be used for numerical simulations as well as for theoretical models. Multiagent copepod diffusion could also be analyzed in these lines, to detect if it provides a realistic enough simulation displaying multifractal statistics.

We have finally proposed a new and simple stochastic model that is able to display such multifractal anomalous diffusion. This process is continuous in time, and in dilatation invariance (in scale), and general enough to include all infinitely divisible models. This model will be studied more thoroughly elsewhere.

Acknowledgements

The authors are indebted to Dr. L. Falk and Dr. H. Vivier for letting us to use their lab facilities (Laboratory of Chemical Engineering Sciences, ENSIC, UPR CNRS 6811, Nancy, France); to Dr. P. Pitiot for his priceless help in the data acquisition and preprocessing; and to Ms. V. Denis for technical assistance. Thanks are also extended to the captain and the crew of the NO 'Sepia II' for their help during the sampling experiments, and to Prof. Y. Lagadeuc for initiating the collaboration with the Laboratory of Chemical Engineering Sciences.

References

[1] W.J. Bell, Searching Behavior, the Behavioral Ecology of Finding Resources, Chapman & Hall, New York, 1991.
[2] P. Turchin, Quantitative Analysis of Movement, Sinauer Associates, Sunderland, MA, 1998.
[3] S. Boinski, P.A. Garber, On the move, how and why animals travel in groups, The University of Chicago Press, Chicago, 2000.
[4] B.T. de Stasio, N. Nibbelink, P. Olsen, Diel vertical migration and global climate change: a dynamic modeling approach to zooplankton behavior, Verh. Int. Verein Limnol. 25 (1993) 401–405.
[5] Z.S. Kolber, F.G. Plumley, A.S. Lang, J.T. Beatty, R.E. Blankenship, C.L. VanDover, C. Vetriani, M. Koblizek, C. Rathgeber, P.G. Falkowski, Contribution of aerobic photoheterotrophic bacteria to the carbon cycle in the ocean, Science 292 (2001) 2492–2495.
[6] R.B. Rivkin, L. Legendre, Biogenic carbon cycling in the upper ocean: effects of microbial respiration, Science 291 (2001) 2398–2400.
[7] H. Jiang, C. Meneveau, T.R. Osborn, Numerical study of the feeding current around a copepod, J. Plankton Res. 21 (1999) 1391–1421.
[8] P. Turchin, Translating foraging movements in heterogeneous environments into the spatial distribution of foragers, Ecology 72 (1991) 1253–1266.
[9] A.R. Johnson, B.T. Milne, J.A. Wiens, Diffusion in fractal landscapes: simulations and experimental studies of tenebrionid beetle movements, Ecology 73 (1992) 1968–1983.
[10] R.S. Wilson, J.O.B. Greaves, The evolution of the bugsystem: recent progress in the analysis of bio-behavioral data, in: F.S. Jacoff (Ed.), Advances in Marine Environmental Research. Proceedings of the Symposium of US EPA (EPA-600/9-79-035), 1979, pp. 251–272.
[11] B. Mandelbrot, The Fractal Geometry of Nature, Freeman, New York, 1983.
[12] S. Frontier, Applications of fractal theory to ecology, in: P. Legendre, L. Legendre (Eds.), Developments in Numerical Ecology, Springer, Berlin, 1987, pp. 335–378.
[13] M. Dicke, P.A. Burrough, Using fractal dimensions for characterizing tortuosity of animal trails, Physiol. Entomol. 13 (1988) 393–398.
[14] J.A. Wiens, B.T. Milne, Scaling of 'landscapes' in landscape ecology, or landscape ecology from a beetle's perspective, Landsc. Ecol. 3 (1989) 87–96.
[15] A.R. Johnson, J.A. Wiens, B.T. Milne, T.O. Crist, Animal movements and population dynamics in heterogeneous landscapes, Landsc. Ecol. 7 (1992) 63–75.
[16] J.A. Wiens, T.O. Crist, K.A. With, B.T. Milne, Fractal patterns of insect movement in microlandscape mosaics, Ecology 76 (1995) 663–666.
[17] K.A. With, Using fractal analysis to assess how species perceive landscape structure, Landsc. Ecol. 9 (1994) 25–36.
[18] K.A. With, Ontogenetic shifts in how grasshoppers interact with landscape structure: an analysis of movement patterns, Funct. Ecol. 8 (1994) 477–485.
[19] D.B. Siniff, C.R. Jenssen, A simulation model of animal movement patterns, Adv. Ecol. Res. 6 (1969) 185–219.
[20] M.L. Cody, Finch flocks in the Mohave desert, Theor. Popul. Biol. 2 (1971) 142–158.
[21] G.H. Pyke, Optimal foraging in hummingbirds: rule of movement between inflorescences, Anim. Behav. 29 (1981) 882–896.
[22] C.R. Gallistel, A.E. Cramer, Computations on metric maps in mammals: getting oriented and chosing a multi-destination route, J. Exp. Biol. 199 (1996) 211–217.
[23] J. Bascompte, C. Vilà, Fractals and search paths in mammals, Landsc. Ecol. 12 (1997) 213–221.
[24] V. Van Ballemberghe, Extraterritorial movements and dispersal of wolves in southcentral Alaska, J. Mammal. 64 (1983) 168–171.
[25] C.M. Bergman, J.A. Schaefer, S.N. Luttich, Caribou movement as a correlated random walk, Ocecology 123 (2000) 364–374.
[26] D.W. Sims, Filter-feeding and cruising speeds of basking sharks compared with optimal models: they filter-feed slower than predicted for their size, J. Exp. Mar. Biol. Ecol. 249 (2000) 65–76.
[27] D.W. Sims, V.A. Quayle, Selective foraging behaviour of basking sharks on zooplankton in a small-scale front, Nature 393 (2001) 460–464.
[28] L. Dagorn, P. Bach, E. Josse, Movement pattern of large bigeye tuna (*Thunnus obesus*) in the open ocean, determined using ultrasonic telemetry, Mar. Biol. 136 (2000) 361–371.

[29] G.C. Hays, C.R. Adams, A.C. Broderick, B.J. Godley, D.J. Lucas, J.D. Metcalfe, A.A. Prior, The diving behaviour of green turtles at Ascension Island, Anim. Behav. 59 (2000) 577–586.
[30] J.Y. Georges, F. Bonadonna, C. Guinet, Foraging habitat and diving activity of lactating Subantarctic fur seals in relation to sea-surface temperature at Amsterdam Island, Mar. Ecol. Prog. Ser. 196 (2000) 291–304.
[31] A. Catard, H. Weimerkirch, Y. Cherel, Exploitation of distant Antarctic waters and close shelf-break waters by white-chinned petrels rearing chicks, Mar. Ecol. Prog. Ser. 194 (2000) 249–261.
[32] G.K. Davoren, A.E. Burger, Differences in prey selection and behaviour during self-feeding and chick provisioning in rhinoceros auklets, Anim. Behav. 58 (1999) 853–863.
[33] Y. Tremblay, Y. Cherel, Benthic and pelagic dives: a new foraging behaviour in rockhopper penguins, Mar. Ecol. Prog. Ser. 204 (2000) 257–267.
[34] M. Burrows, K. Kawai, R.N. Hughes, Foraging by mobile predators on a rocky shore: underwater TV observations of movements of blennies *Lipophrys pholis* and crabs *Carcinus maenas*, Mar. Ecol. Prog. Ser. 187 (1999) 237–250.
[35] J.R. Strickler, J.S. Huang, Matched spatial filters in long working distance microscopy of phase objects, in: P.C. Cheng, J.S. Hwang, J.L. Wu, G. Wang, H. Kim (Eds.), Focus on Multidimensional Microscopy, World Scientific, Singapore, 1999, pp. 217–239.
[36] J.R. Strickler, Observing free-swimming copepods mating, Philos. Trans. Roy. Soc. London B 353 (1998) 671–680.
[37] P. Tiselius, P.R. Jonsson, Foraging behavior of six calanoid copepods: observations and hydrodynamic analysis, Mar. Ecol. Prog. Ser. 66 (1990) 23–33.
[38] D.J. Coughlin, J.R. Strickler, B. Sanderson, Swimming and search behaviour in clownfish, *Amphiprion perideraion*, larvae, Anim. Behav. 44 (1992) 427–440.
[39] L.A. van Duren, J.J. Videler, Swimming behaviour of development stages of the calanoid copepod *Temora longicornis* at different food concentrations, Mar. Ecol. Prog. Ser. 126 (1995) 153–161.
[40] R. Fisher, D.R. Bellwood, S.D. Job, Development of swimming abilities in reef fish larvae, Mar. Ecol. Prog. Ser. 202 (2000) 163–173.
[41] J. Titleman, Swimming and escape behavior of copepod nauplii: implications for predator–prey interactions among copepods, Mar. Ecol. Prog. Ser. 213 (2001) 203–213.
[42] P. Tiselius, Behavior of Acartia tonsa in patchy food environments, Limnol. Oceanogr. 37 (1992) 1640–1651.
[43] M.H. Bundy, T.F. Gross, D.J. Coughlin, J.R. Strickler, Quantifying copepod searching efficiency using swimming pattern and perceptive ability, Bull. Mar. Sci. 53 (1993) 15–28.
[44] N.A. Dowling, S.J. Hall, J.G. Mitchell, Foraging kinematics of barramundi during early stages of development, J. Fish Biol. 57 (2000) 337–353.
[45] L.A. van Duren, J.J. Videler, The trade-off between feeding mate seeking and predator avoidance in copepods: behavioural responses to chemical cues, J. Plankton Res. 18 (1996) 805–818.
[46] P. Tiselius, P.R. Jonsson, S. Karrtvedt, E.M. Olsen, T. Jorstad, Effects of copepod foraging behavior on predation risk: an experimental study of the predatory copepod *Pareuchaeta norvegica* feeding on *Acartia clausi* and *A. tonsa* (Copepoda), Limnol. Oceanogr. 42 (1997) 164–170.
[47] M.C. Brewer, Mating behaviours of *Daphnia pulicaria*, a cyclic parthenogen: comparisons with copepods, Philos. Trans. Roy. Soc. London B 353 (1998) 805–815.
[48] J.R. Strickler, Observing free-swimming copepods mating, Philos. Trans. Roy. Soc. London B 353 (1998) 671–680.
[49] J. Yen, J.R. Strickler, Advertisement and concealment in the plankton: what makes a copepod hydrodynamically conspicuous, Invert. Biol. 115 (1996) 191–205.
[50] T. Gries, K. Jöhnk, D. Fields, J.R. Strickler, Size and structure of 'footprints' produced by Daphnia: impact of animal size and density gradients, J. Plankton Res. 21 (1999) 509–523.
[51] J. Yen, M.J. Weissburg, M.H. Doall, The fluid physics of signal perception by mate-tracking copepods, Philos. Trans. Roy. Soc. London B 353 (1998) 787–804.
[52] M.J. Weissburg, M.H. Doall, J. Yen, Following the invisible trail: kinematic analysis of mate-tracking in the copepod *Temora longicornis*, Philos. Trans. Roy. Soc. London B 353 (1998) 707–712.
[53] J.H. Costello, J.R. Strickler, C. Marrasé, G. Trager, R. Zeller, A.J. Freize, Grazing in a turbulent environment: behavioral response of a calanoid copepod, *Centropages hamatus*, Proc. Natl. Acad. Sci. USA 87 (1990) 1648–1652.

[54] C. Marrasé, J.H. Costello, T. Granata, J.R. Strickler, Grazing in a turbulent environment: energy dissipation, encounter rates, and efficacy of feeding currents in *Centropages hamatus*, Proc. Natl. Acad. Sci. USA 87 (1990) 1653–1657.
[55] J.S. Hwang, J.R. Strickler, Effects of periodic turbulent events upon escape responses of a calanoid copepod, *Centropages hamatus*, Bull. Plankton Soc. Jpn. 41 (1994) 117–130.
[56] J.S. Hwang, J.H. Costello, J.R. Strickler, Copepod grazing in turbulent flow: elevated foraging behavior and habituation to escape responses, J. Plankton Res. 16 (1994) 421–431.
[57] P.R. Jonsson, M. Johansson, Swimming behaviour, patch exploitation and dispersal capacity of a marine benthic ciliate in flume flow, J. Exp. Mar. Biol. Ecol. 215 (1997) 135–153.
[58] P. Larsson, O.T. Kleiven, Food search and swimming speed in *Daphnia*, in: P.H. Lenz, D.K. Hartline, J.E. Purcell, D.L. Macmillan (Eds.), Zooplankton: Sensory Ecology and Physiology, Gordon-Breach, Amsterdam, 1996, pp. 375–387.
[59] V. Kostylev, J. Erlandson, K. Johannesson, Microdistribution of the polymorphic snail *Littorina saxatilis* (Olivi) in a patchy rocky shore habitat, Ophelia 47 (1997) 1–12.
[60] M.E. Ritchie, Scale-dependent foraging and patch choice in fractal environments, Evol. Ecol. 12 (1998) 309–330.
[61] R. Daan, Factors controlling the summer development of the copepod populations in the southern bight of the North Sea, Neth, J. Sea Res. 23 (1989) 305–322.
[62] H.G. Dam, W.T. Peterson, Seasonal contrasts in the diel vertical distribution feeding behavior and grazing impact of the copepod *Temora longicornis* in Long Island Sound, J. Mar. Res. 51 (1993) 561–594.
[63] L. Seuront, F. Schmitt, Y. Lagadeuc, Turbulence intermittency, small-scale phytoplankton patchiness and encounter rates in plankton: where do we go from here?, Deep-Sea Res. 48 (2001) 1199–1215.
[64] I.S. Aranson, M.I. Rabinovich, L.S. Tsimring, Anomalous diffusion of particles in regular fields, Phys. Lett. A 151 (1990) 523–528.
[65] A.S. Pikovsky, Statistical properties of dynamically generated anomalous diffusion, Phys. Rev. A 43 (1991) 3146–3148.
[66] K. Sneppen, M.H. Jensen, Multidiffusion in critical dynamics of strings and membranes, Phys. Rev. E 49 (1994) 919–922.
[67] B.A. Carreras, V.E. Lynch, D.E. Newman, G.M. Zaslasvsky, Anomalous diffusion in a running sandpile model, Phys. Rev. E 60 (1999) 4770–4778.
[68] G.M. Zaslavsky, Multifractional kinetics, Physica A 288 (2000) 431–443.
[69] P. Castiglione, A. Mazzino, P. Muratore-Ginanneschi, A. Vulpiani, On strong anomalous diffusion, Physica D 134 (1999) 75–93.
[70] K.H. Andersen, P. Castiglione, A. Mazzino, A. Vulpiani, Simple stochastic models showing strong anomalous diffusion, Eur. Phys. J. B 18 (2000) 447–452.
[71] P. Castiglione, A. Mazzino, P. Muratore-Ginanneschi, Numerical study of strong anomalous diffusion, Physica A 280 (2000) 60–68.
[72] R. Ferrari, A.J. Manfroi, W.R. Young, Strongly and weakly self-similar diffusion, Physica D 154 (2001) 111–137.
[73] E. Bacry, J. Delour, J.-F. Muzy, A multifractal random walk, Phys. Rev. E 64 (2001) 26 103–26 106.
[74] M.F. Schlesinger, G.M. Zaslavsky, U. Frisch (Eds.), Levy Flights and Related Topics in Physics, Springer, Berlin, 1995, 347pp.
[75] R. Metzger, J. Klafter, The random walk's guide to anomalous diffusion: a fractional dynamics approach, Phys. Rep. 339 (2000) 1–77.
[76] C. Marguerit, D. Schertzer, F. Schmitt, S. Lovejoy, Copepod diffusion within multifractal phytoplankton fields, J. Mar. Syst. 16 (1998) 69–83.
[77] U. Frisch, Turbulence, the Legacy of A.N. Kolmogorov, Cambridge University Press, Cambridge, 1995.
[78] D. Schertzer, S. Lovejoy, F. Schmitt, Y. Chigirinskaya, D. Marsan, Multifractal cascade dynamics and turbulent intermittency, Fractals 5 (1997) 427–471.
[79] A.W. Leising, P.J.F. Franks, Copepod vertical distribution within a spatially variable food source: a simple foraging-strategy model, J. Plankton Res. 22 (2000) 999–1024.
[80] W. Feller, An Introduction to Probability Theory and its Applications, Vol. 1 and 2, Wiley, New York, 1971.
[81] A. Juneja, D.P. Lathrop, K.R. Sreenivasan, G. Stolovitzky, Synthetic turbulence, Phys. Rev. E 49 (1994) 5179–5194.

[82] L. Biferale, G. Boffetta, A. Celani, A. Crisanti, A. Vulpiani, Mimicking a turbulent signal: sequential multiaffine processes, Phys. Rev. E 57 (1998) R6261–R6264.
[83] L. Seuront, F. Schmitt, Y. Lagadeuc, D. Schertzer, S. Lovejoy, Universal multifractal analysis as a tool to characterize multiscale intermittent patterns: example of phytoplankton distribution in turbulent coastal waters, J. Plankton Res. 21 (1999) 877–922.
[84] C.J. Loose, Daphnia diel vertical migration behavior: response to vertebrate predator abundance, Arch. Hydrobiol. Beih. 39 (1993) 29–36.
[85] M. Pascual, F.A. Ascioti, H. Caswell, Intermittency in the plankton: a multifractal analysis of zooplankton biomass variability, J. Plankton Res. 17 (1995) 1209–1232.
[86] L. Seuront, Y. Lagadeuc, Multiscale patchiness of the calanoid copepod Temora longicornis in a turbulent sea, J. Plankton Res. (2001) 23, in press.